JACS
JOURNAL OF THE AMERICAN CHEMICAL SOCIETY

ARTICLE

pubs.acs.org/JACS

Mechanism of Membrane Interaction and Disruption by α-Synuclein

Nicholas P. Reynolds,[†,||] Alice Soragni,[‡,||] Michael Rabe,[†] Dorinel Verdes,[†] Ennio Liverani,[‡] Stephan Handschin,[§] Roland Riek,[*,‡] and Stefan Seeger[*,†]

[†]Institute of Physical Chemistry, University of Zurich, Winterthurerstrasse 190, 8057 Zurich, Switzerland

[‡]Institute of Physical Chemistry, ETH Zurich, Wolfgang-Pauli Strasse 10, 8093 Zurich, Switzerland

[§]Electron Microscopy Center of the ETH Zurich (EMEZ), Schafmattstrasse 18, 8093 Zurich, Switzerland

Supporting Information

ABSTRACT: Parkinson's disease is a common progressive neurodegenerative condition, characterized by the deposition of amyloid fibrils as Lewy bodies in the substantia nigra of affected individuals. These insoluble aggregates predominantly consist of the protein α-synuclein. There is increasing evidence suggesting that the aggregation of α-synuclein is influenced by lipid membranes and, vice versa, the membrane integrity is severely affected by the presence of bound aggregates. Here, using the surface-sensitive imaging technique supercritical angle fluorescence microscopy and Förster resonance energy transfer, we report the direct observation of α-synuclein aggregation on supported lipid bilayers. Both the wild-type and the two mutant forms of α-synuclein studied, namely, the familiar variant A53T and the designed highly toxic variant E57K, were found to follow the same mechanism of polymerization and membrane damage. This mechanism involved the extraction of lipids from the bilayer and their clustering around growing α-synuclein aggregates. Despite all three isoforms following the same pathway, the extent of aggregation and their effect on the bilayers was seen to be variant and concentration dependent. Both A53T and E57K formed cross-β-sheet aggregates and damaged the membrane at submicromolar concentrations. The wild-type also formed aggregates in this range; however, the extent of membrane disruption was greatly reduced. The process of membrane damage could resemble part of the yet poorly understood cellular toxicity phenomenon in vivo.

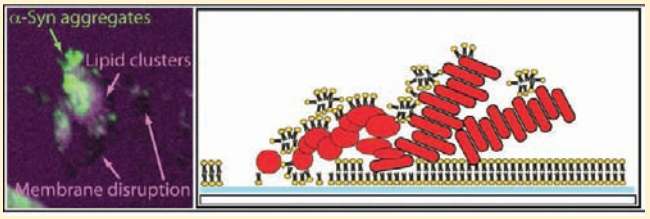

INTRODUCTION

α-Synuclein (α-Syn) is a small, highly conserved protein composed of 140 amino acid residues expressed predominantly in presynaptic terminals in the brain.[1,2] The physiological function of α-Syn remains debatable, but it is thought to play a role in the maintenance of the synaptic vesicle reserve pool of the brain[3,4] and to possess chaperone-like activity for the assembly of soluble NSF attachment protein receptor (SNARE) complexes (NSF = *N*-ethylmaleimide-sensitive factor).[5]

α-Syn is remarkable for its structural variety; in aqueous solutions monomeric α-Syn is reported to be a natively unfolded polypeptide chain, although a recent report from Bartels and co-workers suggests that the physiological conformation is an α-helical folded tetramer.[6] Upon interaction with membrane mimetic detergent micelles, it is folded into a structure containing two antiparallel α-helical regions.[7] Structural studies of α-Syn adsorbed to more physiologically relevant small negatively charged unilamellar vesicles (ULVs) have revealed either similar antiparallel helical structures[8] or alternatively one extended helix.[9,10] α-Syn can also self-aggregate into amyloid fibrils,[11] rich in cross-β-sheet structure. Such large fibrillar aggregates are the major component of Lewy bodies (LBs) found in the intracellular space of neurons and glia cells in the substantia nigra of Parkinson's disease (PD) patients as well as LB dementia (LBD) affected individuals.[12]

The majority of cases of PD are of the late-onset idiopathic type of unknown etiology. In addition, there are rare inherited autosomal dominant cases, which are associated with a gene multiplication of the wild type (WT) or point mutations in the α-Syn gene.[13−16] The first mutant identified was the A53T variant, found in families of Greek and Italian origin.[15] Although in both the idiopathic and familiar PD cases the deposition of the high molecular weight α-Syn aggregates in the neuronal tissue is a ubiquitous pathological feature, there is a growing body of evidence that LBs represent a nontoxic end state and are not directly responsible for the symptoms of the disease.[17−19] However, a recent study indicates that neurons bearing LBs have a shorter life span;[20] therefore, the influence of the presence of LBs remains unclear. Nevertheless, the presently most accepted hypothesis is that soluble or partially soluble oligomeric prefibrillar intermediates arising from the process of aggregation of α-Syn may be the toxic culprits. Insight into the mechanism of toxicity was provided by observing their tight membrane binding[21] and permeabilization[22] of ULVs by α-Syn. This effect was more

Received: April 12, 2011
Published: October 06, 2011

dx.doi.org/10.1021/ja2029848 | *J. Am. Chem. Soc.* 2011, 133, 19366–19375

dramatic for mutant forms of α-Syn compared to the WT.[22] Hypothesized mechanisms of permeabilization include membrane adsorption of α-Syn aggregation intermediates, followed by penetration of the cell membrane forming pores in the bilayer.[22−24] Alternatively, lipid-bound helical α-Syn can cause tubulation of negatively charged vesicular[25] and supported bilayers.[26] This is thought to be related to the suggested physiological vesicle trafficking role of α-Syn; however, excessive tubulation has been shown to cause membrane disruption.[25] In addition, membrane thinning was proposed as a possible toxic mechanism for other amyloidogenic proteins, including Aβ.[27]

Conventionally, interactions between aggregates of α-Syn and lipids are studied by following the adsorption of protein to ULVs in solution and observing the effects by spatially averaging spectroscopic or fluorescent techniques.[22,28] Although this approach has provided valuable knowledge of the interactions of α-Syn with lipids, it does not allow the direct visualization of protein aggregates on the membrane. Supported lipid bilayers (SLBs) are planar fluid membranes formed by the fusion of ULVs onto hydrophilic surfaces. They offer an attractive model for the study of protein aggregation on membranes due to their simplicity compared to cell membranes and their ease of formation on solid supports, making them ideal for use with surface-sensitive imaging techniques. Furthermore, labeling with donor and acceptor fluorophores allows interprotein,[29] intraprotein,[30] and also protein−lipid[31] interactions to be studied by Förster resonance energy transfer (FRET). Traditional microscopy techniques cannot easily distinguish between fluorescence from surface-bound molecules and background signal from fluorophores in the solution. In the work presented here, this disadvantage was overcome using supercritical angle fluorescence (SAF) microscopy, which excludes all fluorescence except that arising from within ∼200 nm of the surface.[32,33] Thus, the adsorption of α-Syn can be studied in real time with no need for washing steps to remove unbound protein from the bulk solution. This approach has previously proven useful in showing time-resolved surface-bound processes for a variety of biomolecules.[29,34,35] Additional to the surface-sensitive imaging, the SAF microscope can simultaneously collect undercritical angle fluorescence (UAF). The images from the UAF channel correspond to those captured from a traditional laser scanning confocal microscope. As with traditional optics, the collection efficiency of the UAF channel extends 2−3 μm into the bulk solution.[33]

Here, SAF was used together with a combined immunostain/dye stain approach to study the behavior of three different variants of α-Syn on the surface of negatively charged SLBs, including the human WT α-Syn, the familial variant A53T, which displays accelerated kinetics of fibril and oligomer formation in vitro[17,36] and also increased toxicity in some animal models,[37] and the designed E57K variant. E57K was shown to be more cytotoxic in a rat model of PD compared to the WT and appears to form more membrane-bound oligomers in vivo than the WT and all familial variants.[38]

EXPERIMENTAL SECTION

Lipid Labeling. 1,2-Dioleoyl-*sn*-glycero-3-phosphoethanolamine (DOPE) in chloroform was used as received (Avanti Polar Lipids). Dy647-*N*-hydroxysuccinimide (NHS) ester dye molecules (Dyomics) were used as fluorescent labels. The DOPE−Dy647 (donor label) complex was formed by the addition of DOPE (7 mg) in chloroform to Dy647-NHS (0.2 mg) in methanol together with 0.05% triethyleneamine (TEA) (Sigma-Aldrich). The resulting mixture was stirred at room temperature for 48 h. The crude reaction product was dried and resuspended in a 1:2:1 mixture of water/chloroform/methanol, and the organic phase containing pure donor-labeled DOPE lipids was extracted. The purity of the labeled lipids was checked by HPLC. The final labeled lipids were stored in chloroform (10 mg mL^{-1}) at −20 °C.

Protein Expression and Purification. The wild-type α-Syn-containing plasmid was a gift of Dr. Goedert (MRC Cambridge). The plasmid was modified by mutating codon 136 from TAC to TAT to avoid cysteine misincorporation at that position.[39] All the mutant plasmids used in the study were generated by site-directed mutagenesis (QuickChangeII, Stratagene) and verified by sequencing.

The protocol followed for protein expression and purification of wild-type and variant α-Syn was adapted from a previous study, with minor modifications discussed in detail in the Supporting Information.[40] Further purification steps of α-Syn were performed as follows: the lyophilized protein was resuspended in cold PBS at a concentration of 2 mg/mL and dialyzed against the same buffer at 4 °C using 3.5 kDa membranes (Slide-A-Lyzer, Pierce). The clear solution was then filtered through a 100 kDa spin filter (Amicon Ultra, Millipore) to remove potential low molecular weight aggregates. It should be noted that small changes to the purification protocol have been shown to result in large variability in aggregation propensity.[38] The protein concentration was adjusted to 1−1.5 mg/mL with PBS at pH 7.4 and the protein kept frozen until needed.

Forming Supported Lipid Bilayers. 1,2-Dioleoyl-*sn*-glycero-3-phospho-L-serine (DOPS) and 1,2-dioleoyl-*sn*-glycero-3-phosphocholine (DOPC) in chloroform (Avanti Polar Lipids) were used as supplied. DOPC, DOPS, and donor-labeled DOPE lipids were combined in appropriate ratios. It was determined that a 1:2500 ratio of DOPE−Dy647 to 65% DOPC/35% DOPS gave an optimum fluorescence intensity in the SAF microscope. The low concentration of fluorophores present in the bilayers is a consequence of the high sensitivity of single photon counting avalanche photodiodes used as detectors in the SAF microscope. The DOPS lipids were added to provide the necessary net negative charge on the bilayer to promote α-Syn binding.[41] The mixture was stirred under reduced pressure to remove the solvent. The resulting solid was placed under high vacuum (10 mbar) overnight to remove any traces of chloroform. The dried lipids were resuspended in membrane buffer (NaCl (100 mM), $CaCl_2 \cdot H_2O$ (3 mM), Tris (10 mM), pH 7.5) (Sigma-Aldrich) and extruded over 40 times through a porous membrane (0.1 μm pore size) to produce ULVs with a homogeneous size distribution.

Solutions of ULVs (0.1 mg mL^{-1}) in membrane buffer were passed through a flow cell (V = 0.2 mL) over a piranha-cleaned (piranha solution is composed of 1 part 35% hydrogen peroxide and 3 parts concentrated sulfuric acid), hydrophilic glass slide. Upon reaching a critical concentration, adsorbed ULVs fuse to form intact SLBs.

Protein Labeling. Cy7-monofunctional NHS ester dye molecules (Amersham) were used as fluorescent labels (acceptor label). Dye to protein coupling was achieved by the addition of 0.2 mg of lyophilized Cy7-NHS to 1 mL of protein solution (∼2 mg mL^{-1}) in PBS buffer at pH between 8 and 9. The mixture was shaken at room temperature for 16−60 h with very similar results in terms of labeling ratios. UV/vis spectroscopy was used to determine dye to protein ratios using the following extinction coefficients: λ_{max}(Cy7) = 747 nm (ε = 250 000 dm^3 mol^{-1} cm^{-1}), λ_{max}(α-Syn) = 280 nm (ε = 5960 dm^3 mol^{-1} cm^{-1}). Ratios between 0.4 and 0.6 were achieved for all proteins. Despite these low labeling ratios, FRET from the fluorescent SLB was still visible in the recorded images. Unreacted dye molecules were separated from labeled proteins via size exclusion chromatography using a Superdex 200 10/300 GL column (Amersham). After labeling, all monomeric protein solutions were stored at concentrations below 50 μM at 4 °C in the dark.

SAF Microscopy. Images of donor-labeled fluorescent bilayers and acceptor-labeled α-Syn were recorded with a custom-made microscope based on SAF detection. The technique uses a parabolic shaped lens to exploit the selective and highly sensitive detection of fluorophores near the dielectric interface, whereas the fluorescence from the bulk solution is collected through a separate optical path allowing for simultaneous collection of surface-sensitive (SAF) and bulk (UAF) fluorescence. See the paper by Verdes et al.[33] for a detailed description of the optical setup. Scans are formed by moving a scanning table of a maximum area of 75 × 75 μm. All measurements were conducted by passing buffered solutions of protein at the desired concentration over the fluorescent SLB through the flow cell with a volume of 200 μL at a constant pump rate of 0.25 mL min^{-1}. The collection of FRET in the SAF channel was made possible by splitting the fluorescence emission into donor and acceptor signals via a dichroic mirror at 730 nm. Donor and acceptor signals were corrected for background emission and for the crosstalk between the two channels.[42] Protein to lipid ratios (p:l) were calculated by estimating the number of lipids occupying the surface area of 6500 mm^2 (which is the surface area of the SLB in the flow cell) and assuming that each lipid headgroup occupies an area of 0.5 nm^2 and dividing this number by the number of α-syn molecules in the volume of the flow cell (flow cell p:l, volume ∼200 μL) or the total amount of protein passing through the flow cell in one experiment (total p:l, volume ∼5 mL). The flow cell p:l varied from 1:4050 (200 nM) to 1:270 (3 μM), and the total p:l varied from 1:21.6 (200 nM) to 1:1.44 (3 μM).

Fluorescence Microscopy. For standard confocal microscopy, the coverslips were removed from the flow cell and applied to a LabTek II borosilicate chamber (Nunc). The samples were kept in PBS buffer, and the pentamer formylthiopheneacetic acid (p-FTAA) dye (1 mg/mL) was filtered through a 0.22 μm filter and added directly to the solution at either 1:500 or 1:1000 dilution. Images were acquired with an inverted Leica DM IRE2 and processed with the Imaris software. To record the emission spectra, series of scans were acquired between 420 and 650 nm with a 10 nm slit when exciting at 405 nm or between 495 and 700 nm when exciting at 488 nm. Intensities of the selected spots were obtained using the Leica LCS software.

Immunofluorescence. For the antibody study, A11 (Invitrogen) and OC (courtesy of Prof. Glabe, University of California, Irvine) antibodies, both raised in rabbit, were directly labeled using the Zenon kit (Invitrogen) according to the manufacturer's instructions. The conjugated A11-Alexa-555 and OC-Alexa-488 resulting antibodies were diluted to either 1:250 or 1:500 in 10% normal goat serum (Sigma-Aldrich) in PBS. The SLBs with or without protein were placed in a four-well Labtek II chamber (Nunc) and incubated with the diluted antibodies for 1 h at room temperature. The samples were then washed twice in PBS and fixed for 15 min with 2% formaldehyde in PBS.

Cryo Scanning Electron Microscopy (Cryo-SEM). Glass coverslips of 10 × 8 mm were precut and extensively washed before being applied to the flow cell. For all the experiments, the protein was flushed at a concentration of 400 nM for 24 h before being removed and washed once in ammonium acetate and three times in doubly distilled water. The coverslips were then plunge frozen in liquid ethane and transferred to the freeze-fracturing system EM BAF 060 (Leica, Vienna, Austria). Freeze-drying was done at −90 °C for 60 min before the sample was coated with 2 nm tungsten at 45° followed by 2 nm at a varying coating angle from 45° to 90°. Cryo-SEM was performed in a field emission SEM instrument, Leo Gemini 1530 (Carl Zeiss, Oberkochen, Germany), equipped with a cold stage to maintain the specimen temperature at −120 °C (VCT Cryostage, Leica, Vienna, Austria). Secondary electrons (SE) (acceleration voltage 5 kV) were used for image formation.

RESULTS

Surface-Bound α-Syn Affects Bilayer Mobility. To investigate the interplay between membranes and α-Syn, the composition of the SLBs was chosen to include a 35 mol % concentration of the anionic phospholipid DOPS to provide a negative charge important for the interaction between membrane and α-Syn.[21,43] Fluorescence recovery after photobleaching (FRAP) measurements were performed on the SLBs before and ∼24 h after protein addition for all three variants (Figure 1) to characterize how the adsorption of α-Syn affects the SLBs. Complete recovery of the fluorescence in the photobleached regions was seen after ∼30 min for the freshly formed SLBs, indicating that the lipids contained within displayed lateral mobility (solid line in Figure 1). However, SLBs showed a significant reduction in mobility upon the adsorption of α-Syn at a concentration of 400 nM. All α-Syn variants studied caused between 40% and 50% reduction in recovery 30 min after bleaching (Figure 1, dashed line). These results indicate that, upon adsorption to the SLBs, α-Syn interacts with the lipids, possibly penetrating the surface of the bilayer and resulting in a reduction of the mobility of the lipids within. The result is in agreement with studies using electron spin resonance (ESR) and polarized infrared spectroscopy, which showed the adsorption of α-Syn causes a reduction in mobility,[44] as well as an ordering of lipids in defect regions of ULVs.[45] The FRAP measurements however do not give insight into the aggregation state of the α-Syn, nor do they resolve any effects specific to individual variants. Therefore, fluorescence microscopy was used to visualize the membrane adsorption of α-Syn and the formation of surface-bound aggregates.

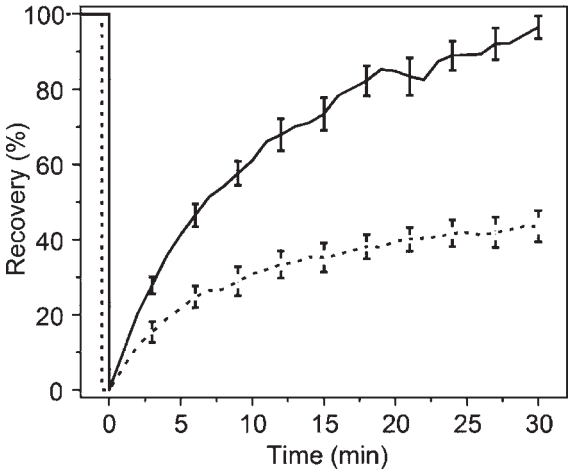

Figure 1. Lipid mobility is decreased by the presence of α-Syn as measured by FRAP. FRAP from donor-labeled SLB before (solid line) and 24 h after (dashed line) adsorption and incubation of 400 nM α-Syn. Photobleaching at time 0′ was achieved using a pulsed laser (635 nm) at an intensity of 1.6 mW for 10 min.

Wild Type and Variants of α-Syn Aggregates on SLBs. In the absence of α-Syn, freshly formed SLBs containing a small fraction of donor-labeled lipids (0.04%) displayed a uniform fluorescence when imaged by SAF microscopy (Figure 2, 0 h). Subsequently, the donor-labeled SLBs were imaged after the addition of a 400 nM solution of monomeric acceptor-labeled α-Syn for 18−24 h. Figure 2 shows representative images of the same area of the bilayer before and at various times after the addition of the three α-Syn variants into the flow cell. For each time point, the fluorescence arising from the donor fluorophores in the bilayer (left column) and from the acceptor fluorophores (center column) and also the FRET efficiencies (right column)

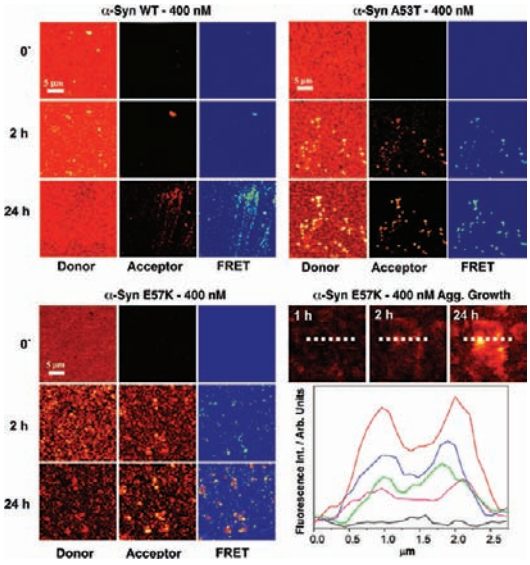

Figure 2. SAF images at different incubation times (0, 2, and 24 h) showing adsorption of three variants of acceptor-labeled α-Syn onto donor-labeled SLBs. For each variant, the left column shows fluorescence from the donor channel of 0−200 (red to yellow) arbitrary units (au), the center column fluorescence from the acceptor channel of 0−50 au (black to red), and the right column FRET intensities of 0−30% (blue to red). The fourth panel shows the evolution of the growth of one aggregate at 1 h (black line), 2 h (pink), 4 h (green), 8 h (blue), and 24 h (red) after injection of α-Syn E57K.

are shown. WT α-Syn had no visible effect on the SLBs at starting concentrations between 100 and 300 nM (Figure S1, Supporting Information). At 400 nM aggregates were clearly visible on the surface of the SLBs after an incubation period of 24 h.

In addition to the WT α-Syn, the effects on aggregation of the familial A53T and the E57K variants were also studied. For the A53T at a concentration of 400 nM, small aggregates appeared in the acceptor and FRET channels within 2 h of protein addition, indicating a rapid formation of aggregates that are closely bound to the SLBs, enabling energy transfer to occur. Indeed, the Förster radius of the Cy7−Dy647 dye pair is 7.13 nm;[29] therefore, at typical FRET efficiencies of 20−30%, the distances between fluorophores were between 8.5 and 9.3 nm. After 24 h the size of the adsorbed aggregates and also the FRET efficiency increased significantly.

A behavior analogous to that of the A53T variant was observed when 400 nM E57K was incubated onto SLBs (Figure 2). After 1−2 h of protein adsorption, the FRET images revealed the appearance of aggregates that continued to grow with the addition of protein, producing large extended structures after 24 h (Figure 2). The cross-section shown in Figure 2 illustrates the growth of one such aggregate over time. The increase in fluorescence intensity shows that after their initial formation on the bilayer the aggregates continue to grow across its surface. It is worth noting that while the aggregates formed within the first 2 h grew over time, new aggregates continued to be formed on the surface of SLBs although with less frequency. This finding indicates that the affinity of α-Syn was higher for the aggregates than for the SLBs (Figure 2). In contrast to A53T and WT, the E57K variant formed visible aggregates on the SLBs at concentrations lower than 400 nM. At concentrations of 200 nM, it was possible to observe clusters of this variant after 2 h (Figure S1, Supporting Information). In summary, at starting concentrations of 200 nM, only the E57K mutant formed visible aggregates on negatively charged SLBs, whereas at 400 nM, aggregation occurred for all variants, but was more pronounced for the two variants.

The concentration of negatively charged lipids is enriched in the inner leaflet of the plasma membrane of most cell types, constituting up to 25 mass % of the total lipids.[46] As α-Syn is a cytosolic protein, it can interact with this class of phospholipids. The composition of the SLBs used in this study was 35 mol % (36 mass %); therefore, to strengthen the argument about the physiological relevance of the present study, we also measured α-Syn aggregation and lipid extraction on the membrane surface with SLBs containing 21 mass % DOPS lipids. Even with the reduced negative charge on the SLB, the effects documented here are still present although less pronounced (Figure S2, Supporting Information).

Surface-Bound α-Syn Aggregates Affect the Bilayer Integrity. Interestingly, an increase in fluorescence intensity was observed in the donor channel at the points of aggregate adsorption. This occurred frequently for both the A53T and E57K variants, but less for the WT (Figure 2). As donor fluorophores were present only on the lipid molecules, this increased fluorescence is attributed to a clustering of negatively charged lipids in the regions of the SLBs where α-Syn aggregates were present. To confirm that this increase in signal was not an artifact of the labeled protein, the experiment was repeated with unlabeled A53T α-Syn. After 24 h, features qualitatively identical to those seen in Figure 2 were observed, indicating that the presence of the label had no influence on lipid clustering (Figure 3a). However, the possibility still remained that the observed clustering was due to an increased affinity of the aggregates for the labeled lipids. To disprove this, the experiment was repeated with SLBs containing different amounts of fluorescently labeled lipids ranging from 0.004% to 1%. When using 0.04% fluorescent lipids or 10 times less fluorophores, 0.004% (Figure 3a and Figure S3, Supporting Information, respectively), the relative increase in fluorescence intensity arising from dye-labeled lipids at α-Syn adsorption sites was always 2−2.5 times greater than the signal from the undamaged SLBs. Similarly, for SLBs containg 1% DOPE−Dy647 (Figure 3b), the relative increase in fluorescence intensity at α-Syn adsorption sites was again between 2 and 2.5 times that of the undamaged regions of the bilayer.

To determine if fluorescence from the clustered lipids was confined to the surface of the bilayer or extended away from the surface, we employed both UAF and SAF channels of the SAF microscope. In the SAF channel we saw the expected increase in fluorescence intensity due to clustered lipids. In the majority of the cases, these features are reproduced in the UAF channel, indicating that the lipids extended into the bulk solution away from the SLB plane (Figure 3a). Despite the sensitivity of the UAF channel being 5 times lower than that of the SAF,[33] the fluorescence from the clustered lipids was more intense in this channel. This increase in intensity is due to lipids absent from the SAF detection volume, which extend away from the plane of the SLB. To further highlight this observation, several confocal plane images at different distances from the SLBs were acquired with a standard confocal microscope. Figure 3b shows two of these confocal planes. The first of these is focused on the surface of labeled SLB imaging aggregates of lipids and protein stained with the Dy647 and amyloid-specific p-FTAA dyes, respectively. The second plane extended 1.6 μm away from the bilayer and clearly showed fluorescence from both aggregates and extracted lipids extending far from the SLB into the solution.

Incubation of WT α-Syn at a starting concentration of 3 μM for 24 h appeared to cause extensive damage to the membrane as

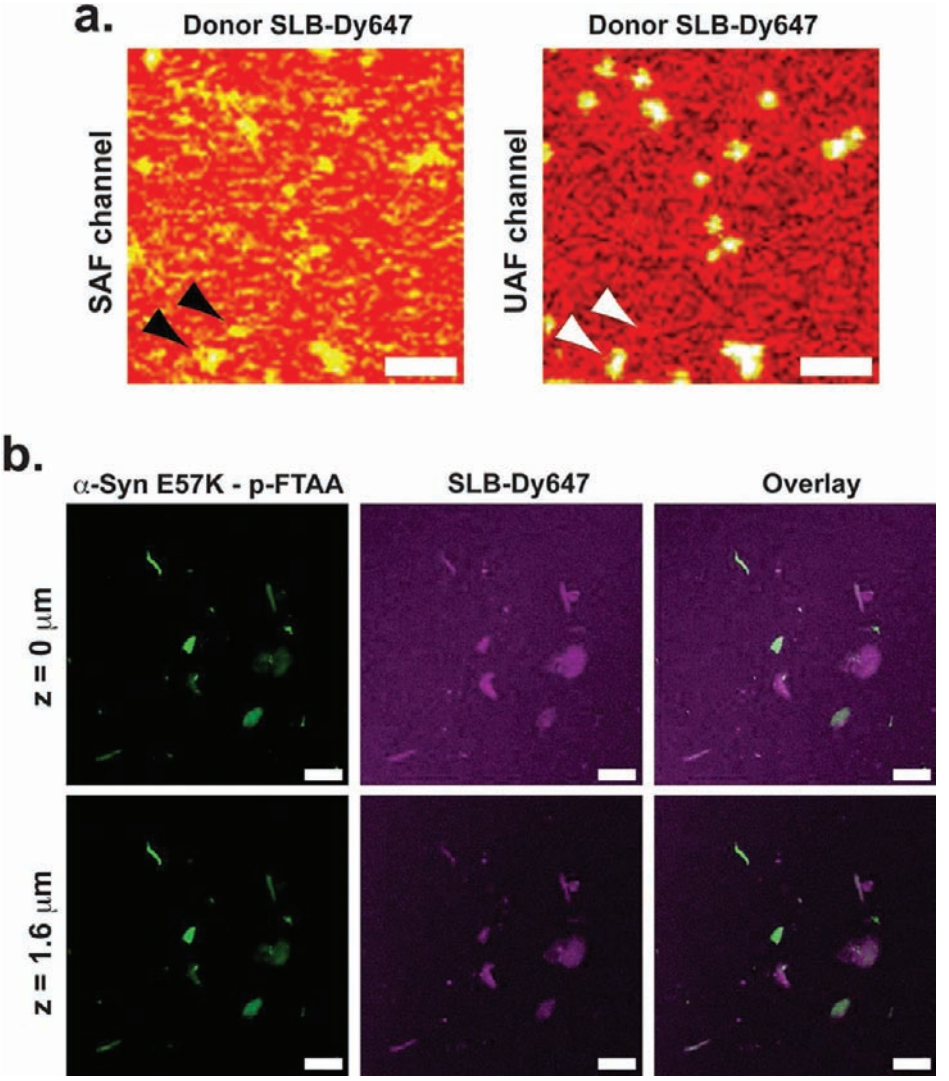

Figure 3. Fluorescence microscopy images showing lipid extraction away from the plane of the SLB. (a) Addition of unlabeled A53T α-Syn (400 nM) to a fluorescent SLB. Most of the aggregates show more intense fluorescence in the UAF channel (top arrows), indicating lipid extraction from the SAF detection volume. The bottom arrows show an area of clustered lipids that is only present in the SAF channel and therefore confined to the surface of the SLB. (b) Confocal images corresponding to different z-planes of a z-stack. The p-FTAA-stained E57K aggregates formed on the SLB at a starting protein concentration of 3 μM (left column) are surrounded by lipids (middle column, lipids labeled with Dy647). The closest plane to the bilayer is indicated as $z = 0$ μm.

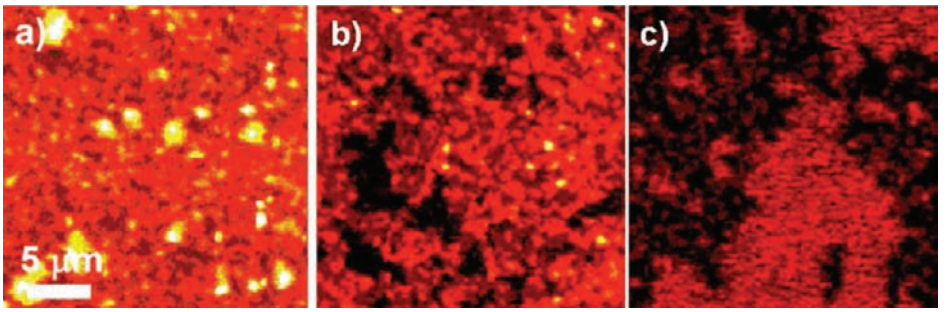

Figure 4. SAF images showing membrane damage to donor-labeled SLBs by WT and E57K α-Syn. (a) and (b) show SLBs 24 h after WT protein incubation of 1.5 and 3 μM, respectively, and (c) shows SLBs 24 h after incubation of a 1.5 μM solution of E57K α-Syn. All images shown on a scale of 0−200 au (black to yellow).

seen by the appearance of dark holes in the SLBs (Figure 4b). Interestingly, the same extent of damage was not observed at 1.5 μM (Figure 4a) for the WT, but was for both the A53T and E57K variants (Figure 4c).

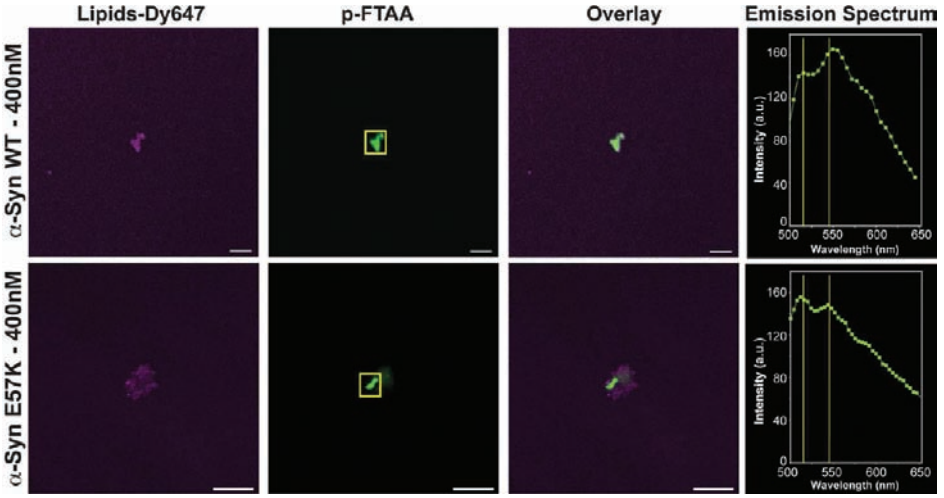

Figure 5. Characterization by confocal microscopy of α-Syn aggregates formed on SLBs. Donor-labeled SLBs were incubated for 24 h with the indicated α-Syn variants before addition of the p-FTAA dye. Emission spectra of fluorescent areas were acquired to confirm the presence of cross-β-sheet-rich entities. For WT α-Syn the excitation wavelength was 405 nm, and for α-Syn E57K, 400 nM, it was 488 nm. The emission spectra were taken from areas highlighted by the yellow boxes. Scale bars indicate 10 μm.

Structural Characterization of the Protein Aggregates. The aggregates present on the SLBs after 24 h of incubation varied in size from a few to tens of micrometers (Figures 2 and 3a). To understand if aggregates from Figures 2 and 3a resembled an end point aggregated state, i.e., mature amyloid fibers, donor-labeled SLBs were flushed with an unlabeled 400 nM protein solution for 24 h as previously described. After this time, the coverslip was removed from the flow cell and transferred into LabTek II borosilicate chambers filled with PBS. Upon addition of the dye p-FTAA, able to bind to mature fibrils and to prefibrillar species,[47,48] the aggregates displayed a characteristic fluorescence (Figure 5; Figure S4, Supporting Information), with emission spectra exhibiting two maxima occurring around 515 and 545 nm typical of amyloid-bound p-FTAA.[47] Additionally, the spectra overlapped well with the emission spectra of α-Syn fibrils grown in solution (Figure S5, Supporting Information). Furthermore, colocalization between the amyloid dye p-FTAA and the donor-labeled lipids was observed (Figure 5), corroborating the SAF data.

To further confirm the amyloid nature of the aggregates, the samples were stained with an Alexa-488-labeled OC antibody,[49] specific to the cross-β-sheet amyloid structure regardless of the primary sequence of the protein of origin (Figure 6).[49] The OC binding further confirmed that the protein aggregates were at least partially composed of mature fibers containing cross-β-sheet structure. The same experiment was measured by SAF microscopy directly in the flow cell with similar results (Figure S6, Supporting Information). This confirms that manipulation of the coverslips (i.e., removal from flow cells, washing steps) did not qualitatively alter the samples, although such handling did result in a loss of SLB-bound aggregates.

To observe the morphology of the adsorbed aggregates with a higher resolution, samples of E57K adsorbed on SLBs were imaged by cryo-SEM, representative images of which are shown in Figure 6 and Figure S7 (Supporting Information) for the negative control. Typical fibril morphologies were observed looking qualitatively identical to fibrils grown under shaking conditions and deposited on clean SLBs (Figure 6). The smaller size of the observed fibrils compared to the SAF data was attributed to the loss of large fibrils during the handling of the coverslips.

To investigate if prefibrillar oligomeric intermediates were also present in the α-Syn aggregates attached to SLBs, immunostaining using the A11 antibody, specific to prefibrillar toxic oligomers,[50] was performed. Indeed, after 24 h of incubation of the E57K variant, a few A11 binding particles were occasionally detected (Figure 6) partially overlapping with the OC-positive spots.

In an attempt to quantify the amount of protein adsorbed to the membrane in a β-sheet conformation, a circular dichroism (CD) experiment was performed. As previously, the experiment was performed in a flow cell, and a 3 or 10 μM solution of WT α-Syn, necessary to gain enough signal in the CD, was washed over the SLB for 24 h. Analysis of the bulk solution reveled that the overwhelming majority of the protein remained in an unstructured conformation in solution (data not shown).

Bilayer Integrity Is Conserved in the Absence of α-Syn Aggregation. To determine the role that amyloidogenic aggregation taking place on the surface of the SLB plays in the process of membrane damage, two additional experiments were performed. First, the experiments in Figure 2 were repeated with the addition of an equimolar amount of dopamine, shown to inhibit α-Syn aggregation.[51,52] Figure 7a illustrates the effect of this experiment when a 400 nM concentration of acceptor-labeled E57K α-Syn was incubated on a donor-labeled SLB in the presence of dopamine. Some clustering of lipids was observed in the donor channel, although much less pronounced than in the absence of dopamine (Figure 2). In addition, there was no evidence of lipid extraction in the UAF channel. Generally, the clustering of lipids was accompanied by a marked increase in the fluorescence in the acceptor channel due to energy transfer from the fluorescently labeled lipids to the aggregating protein (Figure 2). This was not observed in the presence of dopamine (Figure 7a). To exclude the possibility that dopamine prevented the adsorption of α-Syn to the SLB, and therefore the lipid clustering was caused by the dopamine itself, we performed the same experiment in the absence of α-Syn. Dopamine had no effect on the integrity of the SLB after 20 h, and no lipid clustering was observed (Figure 7b). Moreover, the mobility of

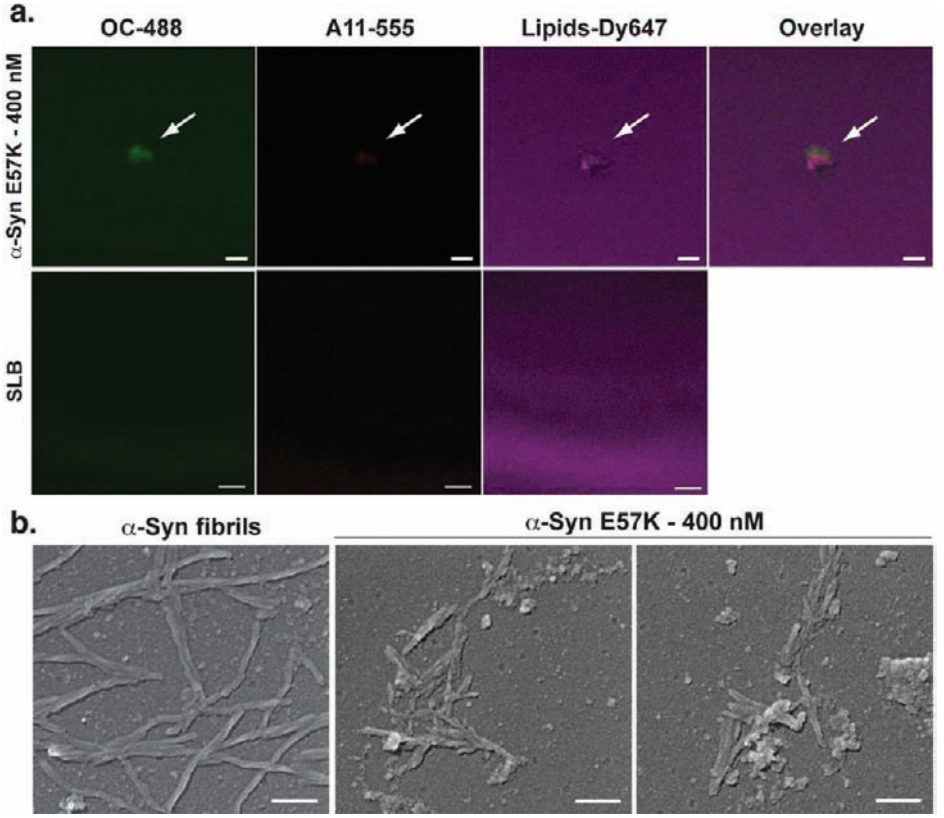

Figure 6. α-Syn E57K aggregates formed on SLBs imaged by (a) immunofluorescence and (b) cryo-SEM. (a) Confocal image of OC and A11 antibodies bound to adsorbed α-Syn E57K on donor-labeled SLBs. The protein clusters formed after 24 h of incubation were stained with the anti-amyloid antibody OC, specific to mature amyloid structures. The same particles were partially recognized by A11, an antibody specific to oligomeric amyloid precursors. SLBs without adsorbed protein were incubated with the same antibodies as a control. Scale bars indicate 2 μm for the E57K sample and 20 μm for the control. (b) Cryo-SEM images of aggregates formed on SLBs after 24 h of incubation with 400 nM E57K α-Syn solution as indicated. The left panel shows a bilayer briefly incubated with α-Syn fibrils aggregated in solution. The two panels to the right show two areas of α-Syn E57K aggregated on the SLB. Scale bars indicate 100 nm.

the lipids within the SLB was reduced in the presence of α-Syn plus dopamine, but not affected in the presence of dopamine alone (Figure 7c), suggesting that α-Syn is still adsorbed to the bilayer.

***α*-Syn Fibers Show No Effect on Donor-Labeled SLBs.** To strengthen the interpretation that protein aggregation on the SLB was responsible for membrane damage, it was tested whether the addition of preformed α-Syn fibers had any effect on donor-labeled SLBs. The addition of 3 μM E57K preformed fibers caused no major perturbation of the membrane as observed in the SAF channel (Figure 7b), although a small amount of lipids were clustered by the bound fibrils (Figure 7b, UAF channel). This observation indicates that the process of aggregation rather than the presence of mature amyloid fibrils is important for membrane damage.

■ DISCUSSION

An aggregated state of the protein α-Syn is believed to cause PD, a neurodegenerative condition characterized by the death of dopaminergic neurons in the substantia nigra[53] and the presence of intracellular α-Syn fibrillar aggregates (LBs).[12] Despite the increasing number of animal models recapitulating one or more features of the disease, and extensive in vitro studies mimicking aggregation, the nature of the toxic α-Syn entity is still under debate. While some studies have found a direct positive correlation between α-Syn fibrillar LBs and cell death,[20] others indicated that fibril formation may not directly induce neurodegeneration.[18] Thus, it was suggested that oligomeric intermediates of α-Syn generated in the process of amyloidogenic aggregation could be the species responsible for cell death.[19,38,54,55] In addition, the mechanism of toxicity is also unknown. It has been proposed that α-Syn oligomers may penetrate the cell membrane, generating voltage-gated channels.[24] Alternatively, the loss of α-Syn function due to aggregation may cause PD.[5,56] Finally, a recent study showed that in vitro the aggregation of α-Syn into amyloid fibrils is driven by physiologically irrelevant air−water interfaces,[57] thus questioning the validity of the current knowledge on α-Syn nucleation and aggregation. In short, the process of α-Syn aggregation, the toxic entity of α-Syn, and the mechanism of toxicity causing PD are not known.

***α*-Syn Aggregates on Membranes.** Toward unraveling some of the questions stated above, the presented study measured the interplay between α-Syn and negatively charged SLBs close to physiological conditions. While the interaction of α-Syn with the membrane initially induces an α-helix-rich structure,[7] here it was observed that in the absence of cellular partners α-Syn self-aggregates on the bilayer at subphysiological concentrations (Figure 2). The majority of the protein however remains unbound from the bilayer in solution as a random coil, as shown by CD. The surface-bound aggregates that are present grow to form micrometer-sized amyloid-like entities, proven by the positive p-FTAA stain (Figures 3 and 5), the OC antibody binding, and

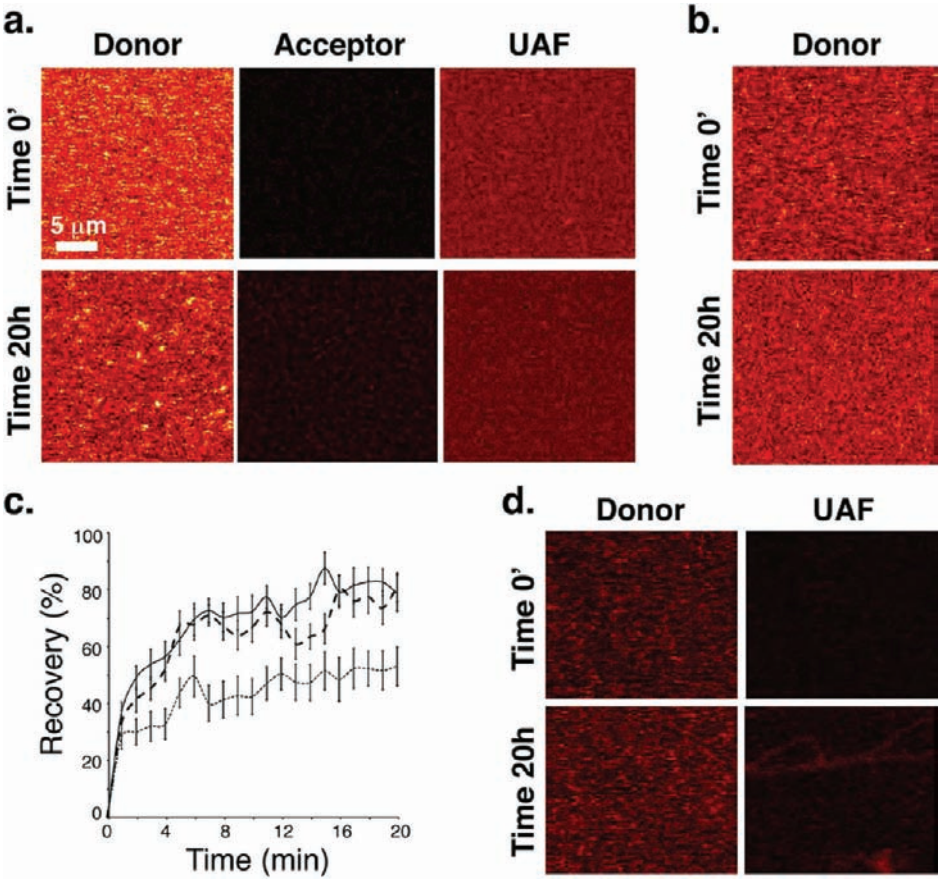

Figure 7. (a) SAF and UAF images showing the adsorption of acceptor-labeled 400 nM E57K α-Syn onto donor-labeled SLBs in the presence of 400 nM dopamine. (b) SAF image of adsorption of dopamine alone on donor-labeled SLBs. (c) FRAP analysis of the lipid mobility of donor-labeled SLBs alone (solid line), donor-labeled SLBs plus 400 nM dopamine after 20 h (large dashes), and donor-labeled SLBs plus 400 nM E57K α-Syn and 400 nM dopamine after 20 h (small dashes). (d) SAF and UAF images of donor-labeled SLBs before and after addition of 3 μM unlabeled E57K preformed fibers. All donor and UAF scans shown on a scale of 0−200 au and all acceptor scans on a scale of 0−50 au.

the cryo-SEM images (Figure 6). Since the established in vitro aggregation process is apparently based on physiologically non-relevant air−water interfaces,[57] it appears that the fast amyloid aggregate formation seen here presents an alternative aggregation pathway of α-Syn including nucleation and aggregation in physiologically relevant conditions.

A Possible Mechanism of Toxicity. When α-Syn begins to aggregate on the SLBs, the growing entities capture lipids from the membrane, resulting eventually (i.e., at higher protein concentration) in membrane disruption. The clustering of the negatively charged lipids at the points of α-Syn aggregation is likely due to a mechanism by which membranous material is extracted from the bilayer by the growing aggregates and transferred to the surface of the growing particles (Figure 8).

The proposed mechanism suggests the extracted lipids seen at lower concentrations may be precursors to more extensive membrane damage resulting in a loss of membrane integrity and/or the formation of pores in the cell membrane, leading to uncontrolled diffusion of molecules in and out of the cell. Indeed, at higher α-Syn concentration, membrane disruption was observed (Figure 4). However, the membrane thinning, transient alterations of its structure, and lateral diffusion properties alone may be sufficient to trigger a cascade of events leading to cell death.[22,23,27,28]

In comparison to that of WT α-Syn, the concentration-dependent process of aggregation and membrane disruption is most pronounced for the highly toxic variant E57K followed by the familial variant A53T. Since A53T α-Syn was shown to be more toxic than WT in mice models[37] and the designed variant E57K caused considerably higher toxicity in a rat model of PD than WT and all the familial mutants,[38] there is a qualitative correlation between in vivo toxicity and bilayer damage caused by α-Syn aggregation presented here. This indicates that the presented measurements offer a simple yet complete mechanism by which the adsorption of α-Syn aggregates may lead to membrane damage sufficient to trigger toxicity and cell death (Figure 8).

The finding that LBs extracted from patients postmortem contained high concentrations of lipids[58] and the presence of lipid-bound oligomers of α-Syn in the brain of normal or α-Syn transgenic mice as well as of PD or LBD patients[59] support the proposed mechanism of α-Syn toxicity to be a major contributing factor to PD pathogenesis. Moreover, it is interesting to note that a similar mechanism of lipid extraction and damage of a bilayer has been observed previously in studies of the aggregation of the type 2 diabetes-associated islet amyloid polypeptide (IAPP) on SLBs.[60]

In our model the extraction of lipids from the surface of the bilayer is due to the amyloidogenic aggregation of α-Syn. Support for this hypothesis arises from the observation that the inhibition of α-Syn aggregation by coincubation with dopamine prevents lipid extraction and membrane damage (Figure 7b),

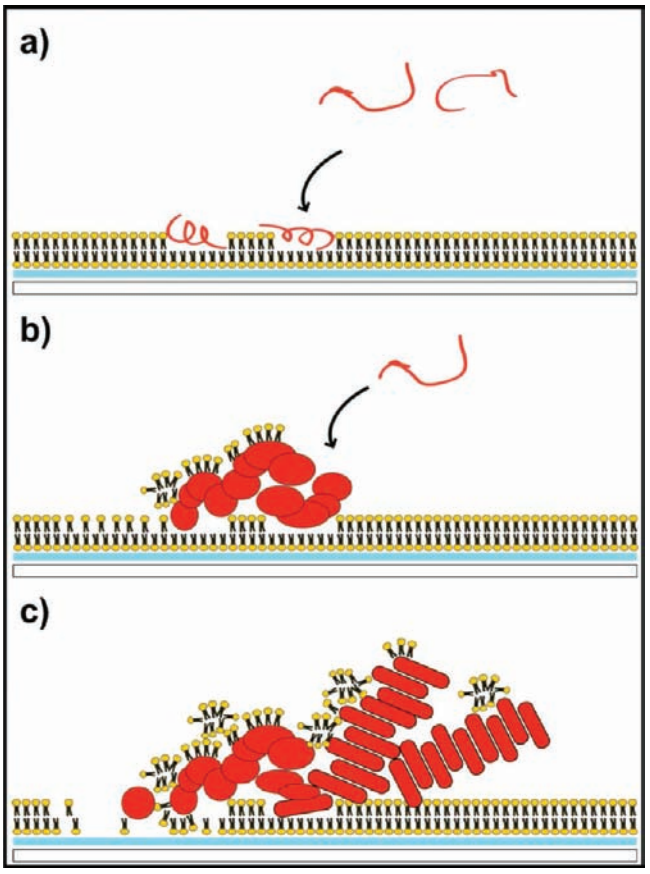

Figure 8. Schematic drawing showing the proposed mechanism of membrane damage caused by aggregation of α-Syn on SLB. (a) Monomeric α-Syn adsorbed to the membrane. (b) Aggregation of α-Syn monomers initiates membrane thinning and lipid extraction around the growing aggregates. (c) A 24 h period of incubation results in the presence of mature α-Syn fibers. Subsequently, membrane integrity is lost.

although FRAP experiments show that the protein still interacts with the SLB (Figure 7c). Dopamine has previously been shown to inhibit α-Syn fibrillation when used at equimolar ratios.[51] This is thought to occur through hydrophobic interactions with the C-terminus of the protein, preventing the formation of mature α-Syn fibrils. However, it was shown that coincubation of α-Syn with dopamine may give rise to small prefibrillar oligomers.[52] The absence of visible protein aggregates in Figure 7a indicates that, in the presence of dopamine, either oligomers are not formed on the SLB or they do not interact with the lipids.

A Possible Origin of Toxicity. As mentioned above, it is still debated which conformational species of α-Syn is primarily responsible for its toxicity. From the above findings, an alternative viewpoint is proposed; instead of one conformation being responsible for toxicity, it could be that the origin of toxicity is the mechanism itself. Once aggregation is initiated, the repetitive structure of the aggregate (i.e., being a repetitive oligomer with a micelle-like structure or an amyloid having the cross-β-sheet motif)[61,62] continuously extracts lipids by aggregate growth. Since this is an intertwined process, the amyloid may be toxic throughout the aggregation process due to repeated cycles of growth and lipid extraction. In contrast, the artificial addition of a fibril to a membrane (or a cell) does not result in severe membrane damage (Figure 7b), as it binds to the surface of the membrane and only extracts a small amount of lipids. A similar scenario may be envisioned for oligomers. When preformed oligomers are added to a membrane or a cell, they may bind to the membrane and either intercalate or extract small amounts of lipids. Such an experiment may result in toxicity;[23] however, it would only partly resemble the toxic mechanism proposed above. In particular, because of the lack of aggregate growth, the extraction of lipids would be limited and the mechanism of aggregation starting from α-Syn monomers adsorbed on the membrane would be missed entirely. Following this argumentation together with the finding that other amyloidogenic proteins were found to aggregate in the presence of lipids,[60] it is likely that also other amyloids associated with diseases may bear in part such a mechanism of toxicity. Indeed, for systemic amyloidosis it has already been proposed that the process of aggregation itself might cause tissue damage, since the removal of the amyloidogenic immunoglobulin light chain abolishes toxicity and causes functional improvement of the affected organs.[63] Similarly, the continuing production of PrP^C is also required for prion toxicity, indicating that also for prion diseases the process of aggregation itself may be the origin of toxicity.[64]

CONCLUSION

In the present study the process of aggregation of WT and two mutant forms of α-Syn on partially negatively charged SLBs was investigated. All three proteins, WT, the familiar variant A53T, and the artificial variant E57K, aggregated when applied on the surface at nanomolar concentrations. Throughout the aggregation process, lipid molecules were extracted from the bilayer by the growing protein aggregates, resulting in membrane thinning. At a micromolar concentration of α-Syn, this process resulted in extensive bilayer disruption. Both the extent of aggregation and the severity of damage to the membrane integrity were correlated with the protein variant applied, with E57K being the most aggressive followed by A53T and WT. We hypothesize that the interplay between growth of the aggregates and lipid extraction reported here could be relevant to the mechanism of toxicity of α-Syn in the case of PD.

ASSOCIATED CONTENT

Supporting Information. Additional methods, SAF microscopy images showing adsorption of WT, A53T, and E57K α-Syn at 200 nM, adsorption of α-Syn to SLBs containing various amounts of fluorophores, adsorption of E57K α-Syn on a 20% DOPS SLB, and OC antibody positive α-Syn aggregates, confocal microscopy images showing p-FTAA staining of α-Syn at 400 nM (A53T) and 3 μM (E57K) and p-FTAA staining of α-Syn fibrils grown in vitro, cryo-SEM image of clean SLBs, and complete refs 13, 15, 38, 47, 55, and 56. This material is available free of charge via the Internet at http://pubs.acs.org.

AUTHOR INFORMATION

Corresponding Author
roland.riek@phys.chem.ethz.ch; sseeger@pci.uzh.ch

Author Contributions
‖These authors contributed equally.

■ ACKNOWLEDGMENT

We kindly acknowledge Dr. Andreas Åslund and Dr. Peter Nilsson (IFM, Linköping University, Linköping, Sweden) for synthesizing p-FTAA. This work was supported by the Swiss National Science Foundation, the University of Zurich, and the ETH.

■ REFERENCES

(1) Iwai, A.; Masliah, E.; Yoshimoto, M.; Ge, N. F.; Flanagan, L.; Desilva, H. A. R.; Kittel, A.; Saitoh, T. *Neuron* **1995**, *14*, 467.
(2) Clayton, D. F.; George, J. M. *Trends Neurosci.* **1998**, *21*, 249.
(3) Cabin, D. E.; Shimazu, K.; Murphy, D.; Cole, N. B.; Gottschalk, W.; McIlwain, K. L.; Orrison, B.; Chen, A.; Ellis, C. E.; Paylor, R.; Lu, B.; Nussbaum, R. L. *J. Neurosci.* **2002**, *22*, 8797.
(4) Murphy, D. D.; Lam, C. L. *Occup. Ther. Int.* **2002**, *9*, 91.
(5) Burrè, J.; Sharma, M.; Tsetsenis, T.; Buchmann, V.; Etherton, M. R.; Südhof, T. C. *Science* **2010**, *329*, 1663.
(6) Bartels, T.; Choi, J. G.; Selkoe, D. J. *Nature* **2011**, *477*, 107.
(7) Bussell, R.; Ramlall, T. F.; Eliezer, D. *Protein Sci.* **2005**, *14*, 862.
(8) Drescher, M.; Veldhuis, G.; van Rooijen, B. D.; Milikisyants, S.; Subramaniam, V.; Huber, M. *J. Am. Chem. Soc.* **2008**, *130*, 7796.
(9) Jao, C. C.; Der-Sarkisson, A.; Chen, J.; Langen, R. *Proc. Natl. Acad. Sci. U.S.A.* **2004**, *101*, 8331.
(10) Jao, C. C.; Hegde, B. G.; Chen, J.; Haworth, I. S.; Langen, R. *Proc. Natl. Acad. Sci. U.S.A.* **2008**, *105*, 19666.
(11) Vilar, M.; Chou, H. T.; Luhrs, T.; Maji, S. K.; Riek-Loher, D.; Verel, R.; Manning, G.; Stahlberg, H.; Riek, R. *Proc. Natl. Acad. Sci. U.S.A.* **2008**, *105*, 8637.
(12) Shults, C. *Proc. Natl. Acad. Sci. U.S.A.* **2006**, *103*, 1661.
(13) Singleton, A. B.; et al. *Science* **2003**, *302*, 841.
(14) Krüger, R.; Kuhn, W.; Müller, T.; Woitalla, D.; Graeber, M.; Kösel, S.; Przuntek, H.; Epplen, J. T.; Schöls, L.; Riess, O. *Nat. Genet.* **1998**, *18*, 106.
(15) Polymeropoulos, M. H.; et al. *Science* **1997**, *276*, 2045.
(16) Zarranz, J. J.; Alegre, J.; Gómez-Esteban, J. C.; Lezcano, E.; Ros, R.; Ampuero, I.; Vidal, L.; Hoenicka, J.; Rodriguez, O.; Atarès, B.; Llorens, V.; Gomez Tortosa, E.; del Ser, T.; Muñoz, D. G.; de Yebenes, J. G. *Ann. Neurol.* **2004**, *55*, 164.
(17) Conway, K. A.; Lee, S. J.; Rochet, J. C.; Ding, T. T.; Williamson, R. E.; Lansbury, P. T. *Proc. Natl. Acad. Sci. U.S.A.* **2000**, *97*, 571.
(18) Goldberg, M. S.; Lansbury, P. T. *Nat. Cell Biol.* **2000**, *2*, E115.
(19) Caughey, B.; Lansbury, P. T. *Annu. Rev. Neurosci.* **2003**, *26*, 267.
(20) Greffard, S.; Verny, M.; Bonnet, A.-M.; Seilhean, D.; Hauw, J.-J.; Duyckaerts, C. *Nuerobiol. Aging* **2010**, *31*, 99.
(21) Pandey, A. P.; Haque, F.; Rochet, J. C.; Hovis, J. S. *Biophys. J.* **2009**, *96*, 540.
(22) Volles, M. J.; Lansbury, P. T. *Biochemistry* **2002**, *41*, 4595.
(23) Lashuel, H.; Petre, B. M.; Wall, J.; Simon, M.; Nowak, R. J.; Walz, T.; Lansbury, P. T. *J. Mol. Biol.* **2002**, *322*, 1089.
(24) Kim, H.-Y.; Cho, M.-K.; Kumar, A.; Maier, E.; Siebenhaar, C.; Becker, S.; Ferandez, C. O.; Lashuel, H.; Benz, R.; Lange, A.; M., Z. *J. Am. Chem. Soc.* **2009**, *131*, 17482.
(25) Varkey, J.; Isas, J. M.; Mizuno, N.; Jensen, M. B.; Bhatia, V. K.; Jao, C. C.; Petrlova, J.; Voss, J. C.; Stamou, D. G.; Steven, A. C.; Langen, R. J. *J. Biol. Chem.* **2010**, *285*, 32486.
(26) Pandey, A. P.; Haque, F.; Rochet, J. C.; Hovis, J. S. *J. Phys. Chem. B* **2011**, *115*, 5886.
(27) Valincius, G.; Heinrich, F.; Budvytyte, R.; Vanderah, D. J.; McGillivray, D. J.; Sokolov, Y.; Hall, J. E.; Lösche, M. *Biophys. J.* **2008**, *95*, 4845.
(28) Volles, M. J.; Lee, S. J.; Rochet, J. C.; Shtilerman, M. D.; Ding, T. T.; Kessler, J. C.; Lansbury, P. T. *Biochemistry* **2001**, *40*, 7812.
(29) Rabe, M.; Verdes, D.; Seeger, S. *Soft Matter* **2009**, *5*, 1039.
(30) Smith, M. L.; Gourdon, D.; Little, W. C.; Kubow, K. E.; Eguiluz, R. A.; Luna-Morris, S.; Vogel, V. *PLoS Biol.* **2007**, *5*, e268.
(31) Antollini, S. S.; Soto, M. A.; de Romanelli, B.; Gutierrez-Merino, C.; Sotomayor, P.; Barrantes, F. J. *Biophys. J.* **1996**, *70*, 1275.
(32) Enderlein, J.; Ruckstuhl, T.; Seeger, S. *Appl. Opt.* **1998**, *38*, 724.
(33) Verdes, D.; Ruckstuhl, T.; Seeger, S. *J. Biomed. Opt.* **2007**, *23*, 034012.
(34) Rabe, M.; Verdes, D.; Zimmermann, J.; Seeger, S. *J. Phys. Chem. B* **2008**, *112*, 13971.
(35) Rabe, M.; Verdes, D.; Rankl, M.; Artus, G. R.; Seeger, S. *ChemPhysChem* **2007**, *8*, 862.
(36) Conway, K. A.; Harper, J. D.; Lansbury, P. T. *Nat. Med.* **1998**, *4*, 1318.
(37) Lee, M. K.; Stirling, W.; Xu, Y.; Xu, X.; Qui, D.; Mandir, A. S.; Dawson, T. M.; Copeland, N. G.; Jenkins, N. A.; Price, D. L. *Proc. Natl. Acad. Sci. U.S.A.* **2002**, *99*, 8968.
(38) Winner, B.; et al. *Proc. Natl. Acad. Sci. U.S.A.* **2011**, *108*, 4194.
(39) Masuda, M.; Dohmae, N.; Nonaka, T.; Oikawa, T.; Hisanaga, S.-I.; Goedert, M.; Hasegawa, M. *FEBS Lett.* **2006**, *580*, 1775.
(40) Volles, M. J.; Lansbury, P. T. *J. Mol. Biol.* **2007**, *366*, 1510.
(41) Davison, S. W.; Jonas, A.; Clayton, D. F.; George, J. M. *J. Biol. Chem.* **1998**, *273*, 9443.
(42) Liu, R.; Hu, D.; Tan, X.; Peter, Lu, H. *J. Am. Chem. Soc.* **2006**, *128*, 10034.
(43) Jo, E.; McLaurin, J.; Yip, C. M.; St George-Hyslop, P.; Fraser, P. E. *J. Biol. Chem.* **2000**, *275*, 34328.
(44) Ramakrishnan, M.; Jensen, P. H.; Marsh, D. *Biochemistry* **2006**, *45*, 3386.
(45) Kamp, F.; Beyer, K. *J. Biol. Chem.* **2006**, *281*, 9251.
(46) Yeung, T.; Grinstein, S. *Immunol. Rev.* **2007**, *219*, 17.
(47) Aslund, A.; et al. *ACS Chem. Biol.* **2009**, *4*, 673.
(48) Hammarström, P.; Simon, R.; Nyström, S.; Konradsson, P.; Aslund, A.; Nilsson, K. P. R. *Biochemistry* **2010**, *49*, 6838.
(49) Kayed, R.; Head, E.; Sarsoza, F.; Saing, T.; Cotman, C. W.; Necula, M.; Margol, L.; Wu, J.; Breydo, L.; Rasool, S.; Gurlo, T.; Butler, P.; Glabe, C. G. *Mol. Neurodegener.* **2007**, *2*, 18.
(50) Kayed, R.; Head, E.; Thompson, J. L.; McIntire, T. M.; Milton, S. C.; Cotman, C. W.; Glabe, C. G. *Science* **2003**, *300*, 486.
(51) Herrera, F. E.; Chesi, A.; Paleologou, K. E.; Schmid, A.; Munoz, A.; Vendruscolo, M.; Gustincich, S.; Lashuel, H.; Carloni, P. *PLoS One* **2008**, *3*, e3394.
(52) Mazzulli, J. R.; Mishizen, A. J.; Giasson, B. I.; Lynch, D. R.; Thomas, S. A.; Nakashima, A.; Nagatsu, T.; Ota, A.; Ischiropoulos, H. *J. Neurosci.* **2006**, *26*, 10068.
(53) Cookson, M. R. *Mol. Neurodegener.* **2009**, *4*, 9.
(54) Danzer, K. M.; Haasen, D.; Karow, A. R.; Moussaud, S.; Habeck, M.; Giese, A.; Kretzchmar, H.; Hengerer, B.; Kostka, M. *J. Neurosci.* **2007**, *27*, 9220.
(55) Karpinar, D. P.; et al. *EMBO J.* **2009**, *28*, 3256.
(56) Cooper, A. A.; et al. *Science* **2006**, *313*, 324.
(57) Pronchik, J.; He, X.; Giurleo, J. T.; Talaga, D. S. *J. Am. Chem. Soc.* **2010**, *132*, 9797.
(58) Gai, W. P.; Yuan, H. X.; Li, X. Q.; Power, J. T. H.; Blumbergs, P. C.; Jensen, P. H. *Exp. Neurol.* **2000**, *166*, 324.
(59) Sharon, R.; Bar-Joseph, I.; Frosch, M. P.; Walsh, D. M.; Hamilton, J. A.; Selkoe, D. J. *J. Neuron* **2003**, *37*, 583.
(60) Domanov, Y. A.; Kinnunen, P. K. J. *J. Mol. Biol.* **2008**, *376*, 42.
(61) Wang, L.; Schubert, D.; Sawaya, M. R.; Eisenberg, D.; Riek, R. *Angew. Chem., Int. Ed.* **2010**, *49*, 3904.
(62) Greenwald, J.; Riek, R. *Structure* **2010**, *18*, 1244.
(63) Bellotti, V.; Mangione, P.; Merlini, G. J. *Struct. Biol.* **2000**, *130*, 280.
(64) Brandner, S.; Isenmann, S.; Raeber, A.; Fischer, M.; Sailer, A.; Kobayashi, Y.; Marino, S.; Weissmann, C.; Aguzzi, A. *Nature* **1996**, *379*, 339.